Published OnlineFirst February 1, 2019; DOI: 10.1158/1078-0432.CCR-18-1940

Precision Medicine and Imaging

Clinical Cancer Research

Exome Analysis Reveals Genomic Markers Associated with Better Efficacy of Nivolumab in Lung Cancer Patients

Corentin Richard[1,2,3], Jean-David Fumet[1,2,3,4], Sandy Chevrier[1,3], Valentin Derangère[1,3], Fanny Ledys[1,2,3], Aurélie Lagrange[4], Laure Favier[4], Bruno Coudert[4], Laurent Arnould[1,3,5], Caroline Truntzer[1,3], Romain Boidot[1,2,3,5,6], and François Ghiringhelli[1,2,3,4,5,6]

Abstract

Purpose: Immune checkpoint inhibitors revolutionized the treatment of non-small cell lung cancer (NSCLC). However, only one-quarter of patients benefit from these new therapies. PD-L1 assessment and tumor mutational burden (TMB) are available tools to optimize use of checkpoint inhibitors but novel tools are needed. Exome sequencing could generate many variables but their role in identifying predictors of response is unknown.

Experimental Design: We performed somatic and constitutional exome analyses for 77 patients with NSCLC treated with nivolumab. We studied: one-tumor-related characteristics: aneuploidy, CNA clonality, mutational signatures, TMB, mutations in WNT, AKT, MAPK, and DNA repair pathways, and two-immunologic characteristics: number of intratumoral TCR clones, HLA types, and number of neoantigens; and six clinical parameters.

Results: A high TMB per Mb, a high number of neoantigens, mutational signatures 1A and 1B, mutations in DNA repair pathways, and a low number of TCR clones are associated with greater PFS. Using a LASSO method, we established an exome-based model with nine exome parameters that could discriminate patients with good or poor PFS ($P < 0.0001$) and overall survival ($P = 0.002$). This model shows better ability to predict outcomes compared with a PD-L1 clinical model with or without TMB. It was externally validated on two cohorts of patients with NSCLC treated with pembrolizumab or with nivolumab and ipilimumab as well as in urothelial tumors treated with atezolizumab.

Conclusions: Altogether, these data provide a validated biomarker that predicts the efficacy of nivolumab or pembrolizumab in patients with NSCLC. Our biomarker seems to be superior to PD-L1 labeling and TMB models.

Introduction

Despite recent advances in the molecular classification of non–small cell lung cancer (NSCLC), the prognosis for advanced patients remains poor (1). Currently patients are treated in first-line with platinum-based chemotherapy or target therapies in case of presence of activating driver mutations. This first-line therapy field is moving rapidly, and for some patients "baseline therapy" will likely be platinum-based chemotherapy combined with immunotherapy in the near future. Despite the effectiveness of these therapies, the prognosis remains poor due to the ineluctable escape of the disease. mAbs targeting "immune" checkpoint inhibitors of the immune response revolutionized the treatment of lung cancer (2, 3). The CheckMate 057 study (4) was the first study demonstrating that an anti-PD-1 antibody (nivolumab) provided a better survival advantage than chemotherapy in lung adenocarcinomas that have progressed after first-line therapy. These data were further confirmed in squamous and nonsquamous cell lung carcinoma treatment using another anti-PD-1 mAb pembrolizumab (5) or the anti-PD-L1 mAb atezolizumab (6). Nivolumab, pembrolizumab, and atezolizumab are currently approved for the second- or third-line treatment of squamous cell carcinoma and adenocarcinoma. Despite the undeniable efficacy of these therapies, only one-quarter of patients with NSCLC benefits from these new therapies (4, 7). Consequently, predictive biomarkers are needed to correctly identify responding patients. The assessment of PD-L1 tumor expression by IHC is used to select responder patients; however, this marker is suboptimal (8, 9) and does not predict the absence of anti-PD-1 efficacy. Despite this shortcoming, PD-L1 remains the gold standard biomarker in many studies (5, 10–12). In addition to histologic markers, transcriptomic and exome analyses have revealed potential biomarkers needing further confirmation (13, 14). Recently, tumor mutational burden (TMB) has emerged as a good surrogate marker of outcome (13, 15). In the Checkmate 026 study of nivolumab use as first-line lung cancer treatment, exploratory analysis also suggests that high TMB is associated with better efficacy of nivolumab compared with chemotherapy (16).

[1]Platform of Transfer in Cancer Biology, France. [2]University of Burgundy Franche-Comté, France. [3]Genetic and Immunology Medical Institute, Dijon, France. [4]Department of Medical Oncology, Georges-Francois LECLERC Cancer Center – UNICANCER, Dijon, France. [5]Department of Tumor Biology and Pathology, Georges François Leclerc Cancer Center - UNICANCER, Dijon, France. [6]INSERM U1231, Dijon, France.

Note: Supplementary data for this article are available at Clinical Cancer Research Online (http://clincancerres.aacrjournals.org/).

C. Truntzer, R. Boidot, and F. Ghiringhelli share co-authorship.

Corresponding Author: François Ghiringhelli, Centre Georges François Leclerc, 1 rue du professeur marion, Dijon 21000, France. Phone: 33380393353; Fax: 33380393434; E-mail: fghiringhelli@cgfl.fr

doi: 10.1158/1078-0432.CCR-18-1940

Published OnlineFirst February 1, 2019; DOI: 10.1158/1078-0432.CCR-18-1940

Translational Relevance

Immunotherapy is a major advance in the treatment of non–small cell lung cancer. However, not all patients benefit from such therapy, so predictive biomarkers are required to improve patients selection. This study demonstrated that exome analysis before initiation of nivolumab therapy can be highly predictive of PFS and OS when analyzed in multiple dimensions. Such analysis is more informative than current biomarkers like PD-L1 or mutation tumor burden. These findings have far-reaching implications for an efficient immunotherapy and should unravel the interest of complex analysis of exome for precision medicine in immuno-oncology.

In this study, we retrospectively performed an analysis of a large set of somatic and constitutional exome parameters in a cohort of patients isolated from the Exoma clinical trial and treated with nivolumab as second- or third-line therapy. The objective was to select biomarkers that better predict nivolumab efficacy compared with previous models.

Materials and Methods

Patients

This prospective monocentric cohort of patients included 77 patients with locally advanced unresectable or metastatic NSCLC treated with nivolumab in monotherapy at the recommended dose (3 mg/kg q2 weeks) in second- or third- line. The patients were treated at Georges-Francois LECLERC Cancer Center. All patients were treated in first-line with platinum-based chemotherapy. They were all prospectively included in the Exoma trial. The clinical data collection and the exome sequencing were performed prospectively according to the trial. The dedicated analysis of this population of patients with NSCLC treated with immunotherapy was performed retrospectively as it was not the aim of the Exoma trial. The database was registered and declared to the National French Commission on Informatics and Liberty (CNIL). The study was conducted in accordance with standard procedures in France and from the Declaration of Helsinki ethical guidelines, with approval from the relevant institutional review boards.

Accordingly, all patients signed a written inform consent before inclusion and benefited from a consultation with a geneticist before constitutional exome analysis. Upon protocol, patients and tumors' characteristics were collected and concerned: age, sex, WHO Performance Status (PS), smoking history, histologic type, tumor stage, EGFR, and Kirsten Rat Sarcoma Viral Oncogene (KRAS) mutation status, anaplastic lymphoma kinase (ALK) rearrangement status, and best RECIST response to nivolumab. All of the CT-scans have been reviewed by two physicians to validate response to nivolumab, and evaluation was based on RECIST 1.1 (17). All progressions were confirmed by a second CT-scan performed 6 weeks after the initial one. The database was closed on August 10, 2017.

Statistical analysis

All patients were followed up until death or the end of data recording (August 10, 2017). Response rate to treatment was assessed by physicians on CT scans using RECIST version 1.1 (17), following 2 months of therapy and patients have been classified in three categories: progression-disease (PD), stable-disease (SD), and partial response (PR). Patients who died early were considered as PD. Progression-free survival (PFS) for nivolumab treatment was calculated as the time from the date of the treatment start to the first recorded evidence of disease progression by the RECIST criteria, clinical evaluation or death, and was censored after 6 months. Overall survival (OS) was calculated as the time from the date of the nivolumab treatment start to the date of death and censored after 24 months. Patients and disease characteristics were examined using the χ^2 test or Fisher exact test for qualitative variables and the Mann–Whitney test or Kruskal–Wallis test for continuous variables, as appropriate. All boxplots were drawn with median, quartiles and Tukey's whiskers. Correlations were estimated with the Spearman's rank correlation coefficient and associated *P*-values were estimated with the cor.test() function from the R package *stats*. Survival probabilities were estimated using the Kaplan–Meier method, best cutoffs for continuous variables were chosen using Cutoff Finder (18) and survival curves were evaluated using the log-rank test. Three multivariate survival models were compared: one model with only clinical variables [gender, age (continuous), WHO performance status, histology and tumor stage] as well as PD-L1 IHC expression called "clinical model"; a second adding TMB per Mb to the first model, called "TMB model"; and a last model, called "exome-derived model", with all exome derived variables selected thanks to a LASSO method using the function *cv.glmnet* from the R package *glmnet* (19). ROC curves were constructed with the linear predictor estimated from each of the previous multivariate models and compared with the function *compareC* from the R package *compare* (20). Statistical analyses were performed using the R software version 3.3.2 and graphs were drawn using GraphPad Prism version 7.03. All tests were two-sided, and *P*-values <0.05 were considered statistically significant.

Data availability

The data sets generated and/or analyzed during this study, as well as the computer code used to perform statistical analysis, are available from the corresponding authors on reasonable request.

Supplementary information about IHC procedures, exome sequencing, and generation of exome-derived variables are available in supplementary methods.

Results

Patient characteristics

Seventy-seven patients with metastatic NSCLC, all of whom were from a single institution (Georges-Francois LECLERC Cancer Center), were included in this analysis. The median follow-up was 11 months. The patients displayed characteristics typical of the metastatic lung cancer population. There were 59 (77%) men and 18 (23%) women. The median age at first nivolumab usage was 66 years old (range, 45–85 years). The most common histologic type was adenocarcinoma ($n = 44$; 57%), which was followed by squamous cell carcinoma ($n = 30$; 39%), and the remaining 4% include two insufficiently differentiated tumors and one neuroendocrine tumor. The population was mostly composed of current or former smokers (70; 91%; Table 1). Median PFS with nivolumab was 2.3 months, and median OS was 13.9 months from metastatic diagnosis. We observed 15 (20%) patients with PR, 18 (23%) patients with SD, and 44 (58%) patients with PD as the best response in accordance with RECIST 1.1 criteria. RECIST

Published OnlineFirst February 1, 2019; DOI: 10.1158/1078-0432.CCR-18-1940

Table 1. Summary of clinical characteristics of the cohort

Variable		RECIST response			
		PD (*N* = *44*)	SD + PR (*N* = *33*)	Total (*N* = *77*)	*P*
Gender, no. (%)	Female	12 (27)	6 (18)	18 (23)	*0.51*
	Male	32 (73)	27 (82)	59 (77)	
Age, years	Median (range)	64 (45–85)	68 (51–85)	66 (45–85)	***0.01***
	Mean (SD)	64.2 (8.4)	69.4 (9.0)	66.4 (9.0)	
Smoker, no. (%)	No	4 (9)	3 (9)	7 (9)	*1.00*
	Yes	40 (91)	30 (91)	70 (91)	
WHO performance status, no. (%)	0	15 (34)	17 (52)	32 (42)	*0.19*
	1–2	29 (66)	16 (48)	45 (58)	
Histology, no. (%)	Nonsquamous cell	25 (57)	19 (58)	44 (57)	*0.97*
	Squamous cell	18 (41)	12 (36)	30 (39)	
	Other	1 (2)	2 (6)	3 (4)	–
Stage, no. (%)	IIIB	4 (9)	6 (18)	10 (13)	*0.31*
	IV	40 (91)	27 (82)	67 (87)	
EGFR, no. (%)	Not mutated	40 (91)	31 (94)	71 (92)	*0.70*
	Mutated	4 (9)	2 (6)	6 (8)	
KRAS, no. (%)	Not mutated	25 (76)	18 (78)	43 (77)	*1.00*
	Mutated	8 (24)	5 (22)	13 (23)	
ALK, no. (%)	Not mutated	31 (100)	19 (95)	50 (98)	–
	Mutated	0 (0)	1 (5)	1 (2)	
	Not evaluated	13	13	26	
PD-L1 expression (Sp142), no. (%)	Low	27 (64)	16 (48)	43 (57)	*0.26*
	High	15 (36)	17 (52)	32 (43)	
	Not evaluated	2	0	2	–

response is strongly associated with PFS [median for PD = 1.7; SD = 4.8; PR = not reached (NR); log-rank test $P < 0.0001$; $n = 77$] and OS (median PD = 9.8; SD = 22.9; PR = NR; log-rank test $P = 0.0008$; $n = 77$; Supplementary Fig. S1A and S1B). PD-L1 staining using Sp142 mAb was observed in 55 patients; a high level of PD-L1 was not significantly associated with better PFS but was associated with a better OS (median OS: 12.1 months vs. 22.8 months; log-rank test $P = 0.03$; $n = 55$; Supplementary Fig. S1C and S1D).

In this group, 65 patients had sufficient blood and tumor tissue to process all somatic and constitutional exome analyses, and for 12 patients, only an estimation of their TCR clonality could be performed because of an absence of constitutional sample (Supplementary Fig. S2).

Association between TMB, mutational signatures, and outcome

We identified a median TMB of 4.1 mutations per Mb (range, 0.6–43.7; Fig. 1A). Using a cutoff of 5.73 mutations per Mb, a higher TMB per Mb was significantly associated with a better PFS (median 4.6 months vs. 2 months, log-rank test $P = 0.03$; $n = 65$; Fig. 1B) but was not associated with OS (median 17.5 months vs. 16.7 months, log-rank test $P = 0.62$; $n = 65$; Supplementary Fig. S3A).

We observed a strong heterogeneity of mutational signatures across patients (Fig. 1C). The most frequently expressed signatures were signature 1A (87%, 54/62) and signature 4 (60%, 37/62). Among the 27 tested signatures, we chose to keep only the most common signatures across patients (frequency > 25%), which are signatures 1A, 1B, 3, 4, 6, 16, and 21. Only signature 4 was significantly correlated with TMB per Mb (Spearman $\rho = 0.50$; $P < 0.0001$; $n = 62$; Fig. 1D), confirming that smoking induces several mutations. When focusing on the prognostic utility of the different signatures, we observed that only signatures 1A and 1B had an influence on PFS (Fig. 1E). A high fraction of signature 1A is associated with a better PFS (median 4.3 months vs. 2 months; log-rank test $P = 0.02$; $n = 62$; Fig. 1F) and with a better OS (median 22.9 vs. 10.3; log-rank test $P = 0.04$; $n = 62$; Supplementary Fig. S3B). A high fraction of signature 1B is associated with a poor PFS (median 1.8 vs. 3.3; log-rank test $P = 0.03$; $n = 62$; Fig. 1G) but not with OS (median 13.3 vs. 17.3; log-rank test $P = 0.93$; $n = 62$; Supplementary Fig. S3C). The other signatures such as signatures related to homologous recombination deficiency or mismatch repair (signatures 3 and 6) or smoking (signature 4) were not significantly associated with any outcome (Supplementary Fig. S3D–S3H).

These data indicate that not only the TMB but also the specific profile of mutations is associated with nivolumab efficacy.

Association between chromosomal instability, tumor clonality, and outcome

Chromosomal instability was previously reported to impact immune response in breast cancer or colorectal cancer (21, 22). The median number of large deletions was 7 (range, 0–19), and the median for large LOH was 17 (range, 1–28). Twenty-six patients were estimated to be aneuploid (41%, 26/63), and one-quarter of patients presented only one major CNA clone (27%, 17/63; Fig. 2A).

Aneuploidy, LOH, CNA clones, and large deletions were all pairwise correlated; only the number of large deletions and the number of CNA clones were not pairwise correlated (Supplementary Fig. S4). However, none of these variables were correlated with TMB, thus suggesting that these variables can provide additional information to TMB.

We observed that high numbers of large LOH and deletions were associated with a poor PFS prognosis (LOH: median 1.7 months vs. 2.6 months; log-rank test $P = 0.02$; deletions: median 1.8 months vs. 3.1 months; log-rank test $P = 0.03$; $n = 63$; Fig. 2B and C), whereas tumor CNA polyclonality and aneuploidy were not associated with PFS (Supplementary Fig. S5A and S5B). Both the high number of large deletions and aneuploidy were significantly associated with reduced OS (deletions: median 9.3 months vs. 22.8 months; log-rank test $P = 0.004$; ploidy: median

Published OnlineFirst February 1, 2019; DOI: 10.1158/1078-0432.CCR-18-1940

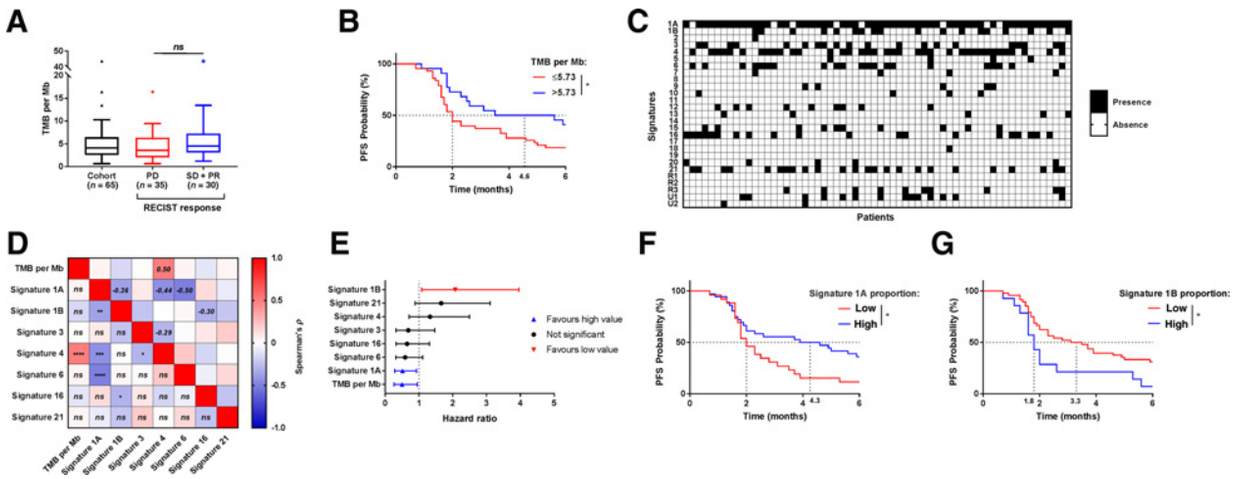

Figure 1.

Prognostic role of tumor burden and mutational signatures. **A,** Boxplots showing the distribution of the TMB per Mb for all patients (in black), patients with progression-disease RECIST response (PD; in red), and pooled patients with stable-disease and partial response (SD + PR; in blue). **B,** Kaplan–Meier estimates of PFS; patients were stratified according to their TMB per Mb: high rate (>5.73; in blue) or low rate (≤5.7; in red). **C,** Heatmap showing the presence/absence of mutational signatures (Alexandrov and colleagues 2013) for each patient. Presence of a mutational signature is represented with a black square, and a white square represents absence of the signature. **D,** Spearman's rank correlation matrix between TMB per Mb and mutational signature proportions. Lower triangular matrix: *P*-values of corresponding correlation test. Upper triangular matrix: Spearman's rank correlation coefficients for significant tests. **E,** Forest plot of the hazard ratios and corresponding 95% confidence intervals estimated from corresponding univariate Cox models: variables significantly associated with a good PFS are displayed in blue, poor PFS variables are in red, and nonsignificant variables are in black. **F–G,** Kaplan–Meier estimates for PFS; patients were stratified according to their proportions of signatures 1A (**F**) and 1B (**G**): low proportion (in red) and high proportion (in blue). All cutoffs were defined with the Cutoff Finder method. *, $P < 0.05$; **, $P < 0.01$; ***, $P < 0.001$; ****, $P < 0.0001$; ns, not significant.

11.9 months vs. 22.9 months; log-rank test $P = 0.01$; $n = 63$). A high number of large LOH and CNA polyclonality approached significance (LOH: median 10.2 months vs. 21.6 months; log-rank test $P = 0.053$; CNA clonality: median 13.7 months vs. 23 months; log-rank test $P = 0.051$; $n = 63$; Supplementary Fig. S5C–S5F).

Together, these data support the hypothesis that a high level of chromosomal instability is associated with poor outcome with nivolumab treatment.

Alterations of genetic pathways and outcome

We studied the prognostic role of the top mutated genes in this cohort. We selected 320 genes that were mutated in more than 10% of the cohort. Cox univariate models indicated that 13 mutated genes were associated with better PFS, whereas eight mutated genes were associated with reduced PFS (data not shown). However, after FDR correction for multitesting, no mutated genes were significantly associated with PFS (data not shown).

To investigate further, we studied the implications of mutations linked to genetic pathways classically activated in lung cancer or previously involved in immunosubversion or resistance to checkpoints in other diseases (23 ,24). We focused on the MAPK, PI3K/AKT, and WNT pathways. The genes involved in these pathways are listed in Table S1. For the MAPK and PI3K/AKT pathways, only somatic mutations were studied. For the WNT pathway, we looked at both somatic and constitutional mutations because these germline alterations have been shown to impact tumor development. Twenty-six percent, 9% and 11% of patients had at least one deleterious mutation involved in the MAPK, PI3K/AKT, and WNT pathways, respectively (Supplementary Fig. S6A). Activating mutations in the MAPK and PI3K/AKT pathways were not associated with PFS (Supplementary Fig. S6B) or with OS (Supplementary Fig. S6C). Mutations in the WNT pathway were only associated with a poor OS (median 21.6 months vs. 6.8 months; log-rank test $P = 0.045$; $n = 65$; Fig. 2D and S6D).

We then addressed the presence of mutations in the DNA repair machinery. We looked at the frequency of mutations in homologous recombination (HR), mismatch repair (MMR), base excision repair (BER), nucleotide excision repair (NER), and nonhomologous end joining (NHEJ) pathways at both the somatic and constitutional levels. We observed that germline mutations were more frequent than somatic mutations, and most mutations were in the HR pathway (Supplementary Fig. S6E). We observed a significant association between TMB per Mb and mutations in DNA repair machinery (for any DNA repair pathway; Wilcoxon rank-sum test $P = 0.03$; $n = 65$; Supplementary Fig. S6F). When looking at the association with prognosis, we first observed that somatic DNA repair machinery mutations were associated with a better PFS with Nivolumab therapy (median PFS: 5 months vs. 2 months; log-rank test $P = 0.01$; $n = 65$; Fig. 2E) but were not associated with OS (median OS: 16.7 months vs. 22.8 months; log-rank test $P = 0.52$; $n = 65$; Supplementary Fig. S6G). Because germline mutations in DNA repair pathways could impact tumor behaviour, we considered the presence of somatic and/or germline mutations in DNA repair pathways. Importantly, presence of at least one somatic or one constitutive mutation improved the ability of this variable to predict PFS (median PFS: 3.9 versus 1.9 months; log-rank test $P = 0.004$; $n = 65$) (Fig. 2F) but not to predict OS (median OS: 16.7 versus 22.8 months; log-rank test $P = 0.23$; $n = 65$) (Supplementary Fig. S6H). DNA repair genes are considered tumor suppressors, and it is presumed that a double

Published OnlineFirst February 1, 2019; DOI: 10.1158/1078-0432.CCR-18-1940

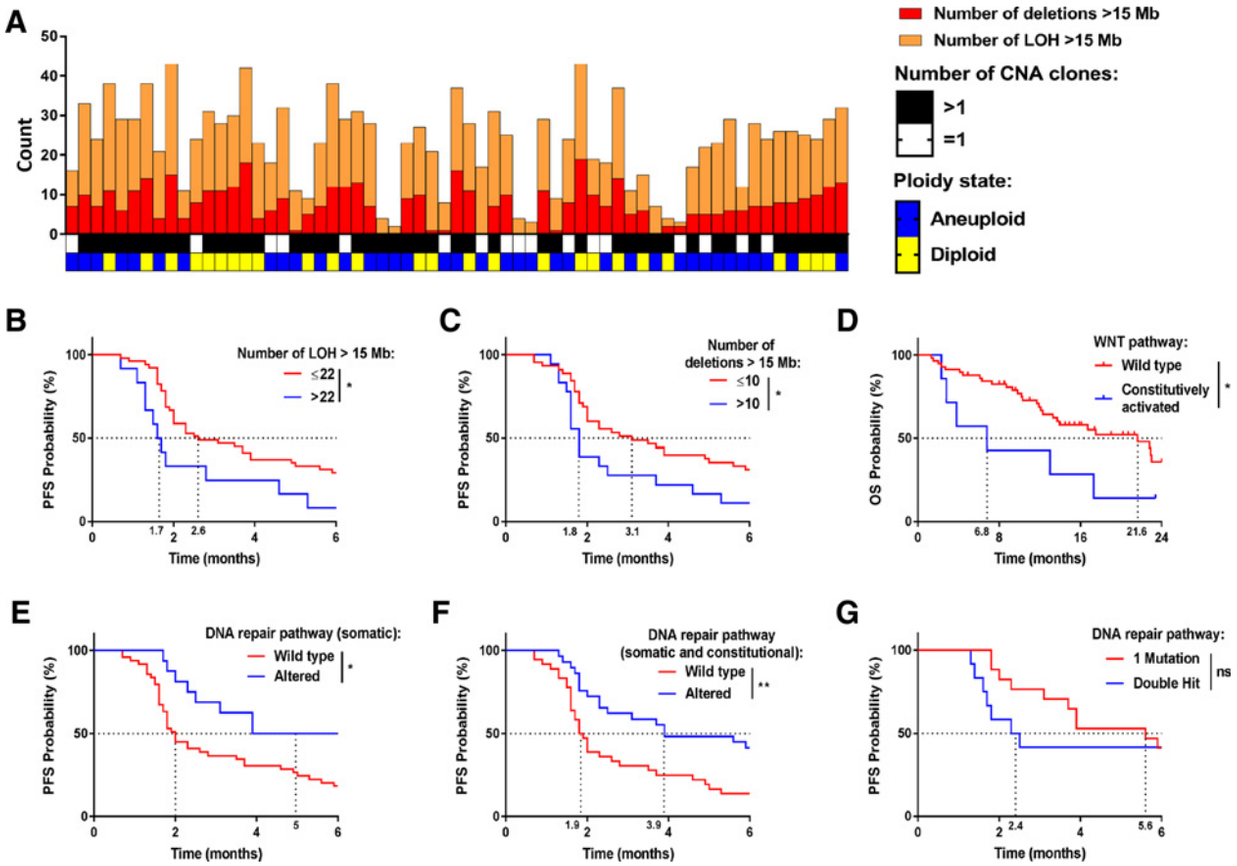

Figure 2.

Prognostic role of tumor chromosomal instability and mutations in oncogenic pathways. **A,** Top: Bar plot showing the number of large (>15 Mb) deletions (in red) and losses of heterozygosity (LOH; in orange) for each patient. Bottom: heat-map showing the number of CNA clones (one clone in white, more than one clone in black) and the tumor ploidy state (diploid in yellow and aneuploid in blue). **B** and **C,** Kaplan–Meier estimates of PFS; patients were stratified according to the number of large LOH (**B**) and the number of large deletions (**C**): high number (in blue) or low number (in red). **D,** Kaplan–Meier estimates for overall survival; patients were stratified according to the presence of mutations in the WNT pathway: wild-type (in red) and presence of activated mutations (in blue). **E** and **F,** Kaplan–Meier estimates for PFS; patients were stratified according to the presence of somatic mutations (**E**) and pooled somatic and constitutional mutations (**F**) in genes involved in the DNA repair pathway: wild-type (in red) and altered (in blue). **G,** Kaplan–Meier estimates for PFS; patients were stratified according to their DNA repair pathway state: single hit (only one mutation; in red) or double hit (in blue), which is at least two mutations or one mutation and one loss of heterozygosity. Only patients with at least one mutation in the DNA repair pathway were retained for this analysis. All cutoffs were defined with the Cutoff Finder method. *, $P < 0.05$; **, $P < 0.01$; ***, $P < 0.001$; ****, $P < 0.0001$; ns, not significant.

hit (germline and somatic alterations or 2 somatic alterations, such as point mutation and loss of heterozygosity) is required for complete pathway inactivation. We observed no significant difference for PFS (Fig. 2G) or OS (Supplementary Fig. S6I) between the 17 patients with a single hit and the 12 patients with a double hit.

Altogether, our data indicate that mutation in WNT oncogenic pathway is associated with poor outcomes, while mutations in DNA repair machinery positively impact nivolumab efficacy.

Association of exome immune parameters with outcome

Because the TMB per Mb is linked to PFS, we decided to examine the landscape of neoantigens using pVACseq software. We identified a median of 22 candidate neoepitopes per tumor (range, 0–236) and observed that the number of neoantigens per tumor was correlated with the tumor mutation burden per Mb (Spearman $\rho = 0.84$; $P < 0.0001$; $n = 65$; Fig. 3A). The absolute burden of candidate neoantigens was strongly associated with a better PFS (median PFS: NR months vs. 2 months, log-rank test $P = 0.004$; $n = 65$; Fig. 3B) but was not associated with OS (median OS: 17.5 months vs. 17.3 months, log-rank test $P = 0.76$; $n = 65$; Supplementary Fig. S7A). Type I HLA phenotype was heterogeneous and sparse (Supplementary Fig. S7B) across patients. Only specific HLA alleles present in at least 25% of patients were further considered, namely, HLA-A*01, HLA-A*02, HLA-A*24, and HLA-C*07. Specific HLA alleles did not correlate with nivolumab efficacy, except HLA-A*01, which was associated with a better OS (Fig. 3C).

In our cohort, TCR clonality was studied using the MixCR software on somatic exome data. The median number of TCR clones detected was 4 (range 0–21). TCR clonality was not associated with TMB per Mb or the number of neoepitopes (Fig. 3D; Supplementary Fig. S7C). A restriction in the number of TCR clones was associated with a good PFS (median PFS: 2.8 vs. 2.1; log-rank test $P = 0.03$; $n = 77$). Using the biological rationale

Published OnlineFirst February 1, 2019; DOI: 10.1158/1078-0432.CCR-18-1940

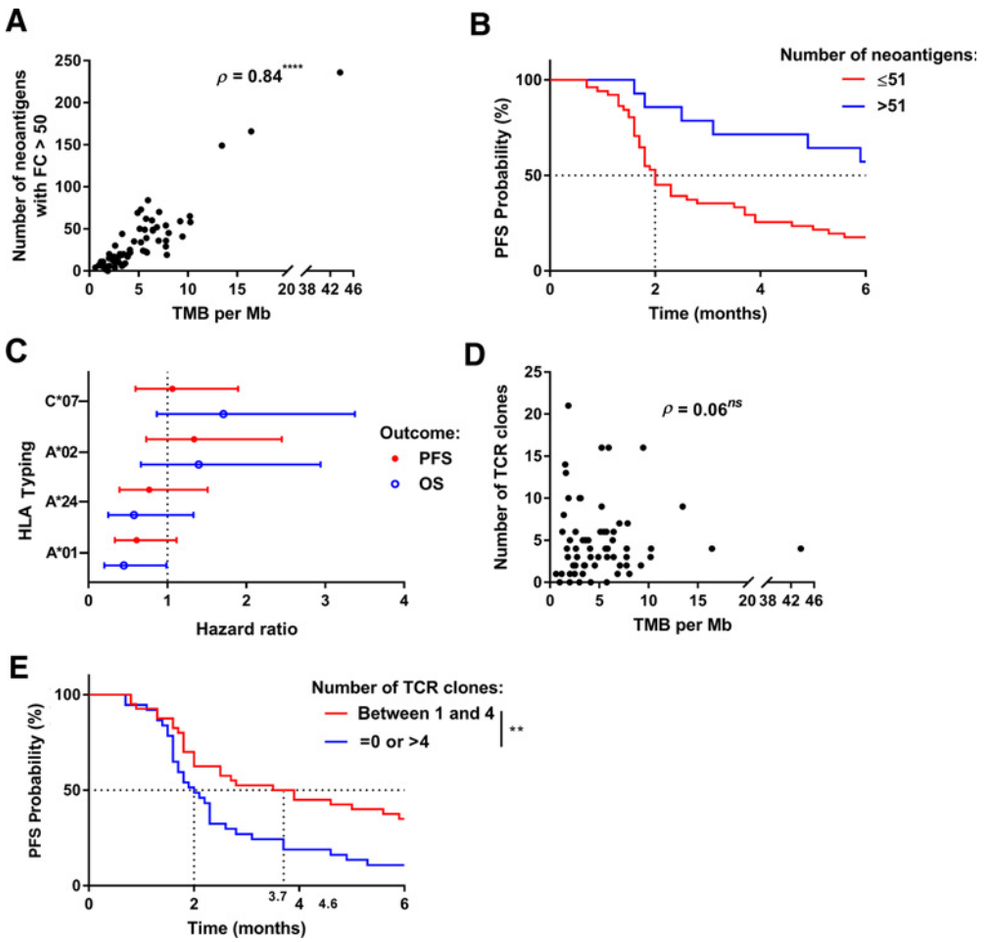

Figure 3.

Prognostic role of immune-related variables. **A,** Scatterplot showing the number of bioinformatically detected neopeptides for a given TMB per Mb. The ρ value represents Spearman's rank correlation. **B,** Kaplan–Meier estimates for PFS; patients were stratified according to their number of neopeptides: low rate ($\leq$51; in red) or high rate (>51; in blue). **C,** Forest plot of the hazard ratios and corresponding 95% confidence intervals estimated for HLA typing from univariate Cox models: considering PFS as outcome in red or OS in blue. **D,** Scatterplots showing the number of bioinformatically detected T-cell receptor (TCR) clones for a given TMB per Mb. The ρ value represents Spearman's rank correlation. **E,** Kaplan–Meier estimates for PFS; patients were stratified according to the number of TCR clones: between 1 and 4 clones (in red), or less than 1 or more than 4 (in blue). All cutoffs were defined with the Cutoff Finder method. *, $P < 0.05$; **, $P < 0.01$; ***, $P < 0.001$; ****, $P < 0.0001$; ns, not significant.

that tumors with poor immunologic responses include tumors with no T-cell infiltration and tumors with polyclonal nonspecific T-cell infiltration, we decided to improve the biological classification by including patients having no TCR clone in the tumor with patients with a high number of TCR clones. We observed that clonal restriction in tumors was associated with a better PFS (median PFS: 2.0 vs. 3.7; log-rank test $P = 0.005$; $n = 77$; Fig. 3E) but not with OS (median OS: 13.3 vs. 21.6; log-rank test $P = 0.11$; $n = 77$; Supplementary Fig. S7D).

Together, these data indicate that a high number of neoepitopes and a restricted number of TCR clones are associated with better outcome.

An exome composite variable is an efficient predictor of a good outcome.

Three multivariate Cox models—clinical, TMB, and exome-derived models—were adjusted with PFS as outcome by survival analyses. One model included all clinical variables (sex, age, WHO performance status, histology, the tumor stage, and smoker state) and PD-L1 IHC expression (Sp142 antibody), one included all previous variables and the TMB per Mb as described in Rizvi and colleagues (14) and the last model included a selection of relevant variables among the 21 exome-derived variables. By using the LASSO algorithm, we selected the following nine variables: the DNA repair pathway status (altered vs. wild-type), the WNT pathway status (altered vs. wild-type), the number of TCR clones, the number of neoantigens, the HLA*A*1, and HLA*A*24 statuses, and the fractions of signatures 1A, 1B, and 6. ROC curves based on the linear predictors for each of the three models estimated on 44 patients for whom all exome-derived and clinical variables were available showed that the exome-derived model was more predictive than the others (clinical vs. exome-derived models AUC: 80.3 vs. 92.3; Z-test $P = 0.003$; TMB vs. exome-derived model AUC: 80.5 vs. 92.3; Z-test $P = 0.01$; $n = 60$; Fig. 4A).

Published OnlineFirst February 1, 2019; DOI: 10.1158/1078-0432.CCR-18-1940

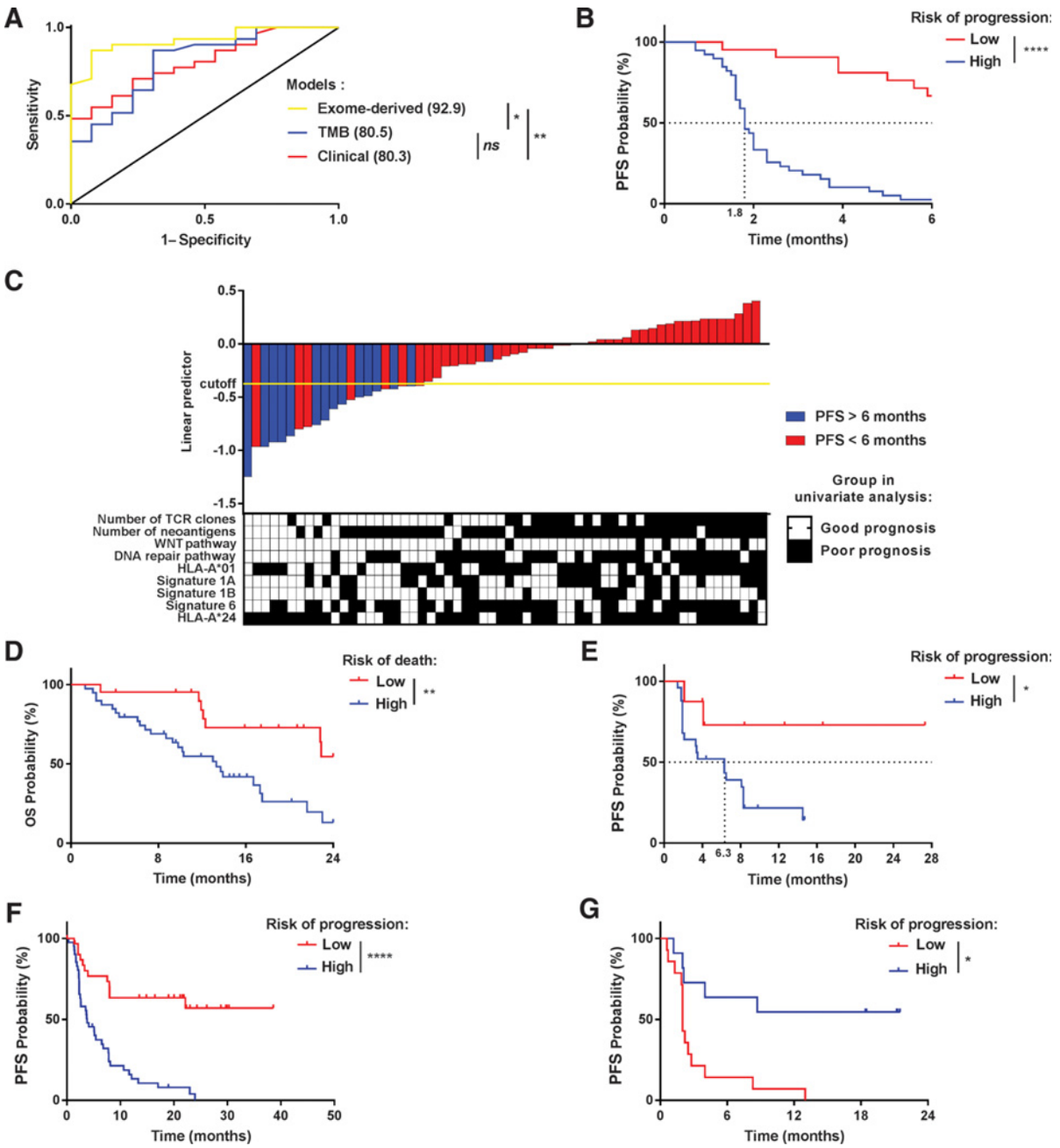

Figure 4.

Prognostic role of the composite exome biomarker. **A,** ROC curves estimated using the linear predictor of the clinical and PD-L1 Cox model (clinical; in red), the clinical and TMB model (in blue), and the exome-derived model (in yellow). For each model, the area under the curve is given in brackets. **B,** Kaplan–Meier estimates for PFS; patients were stratified according to the value of the linear predictor estimated from the exome-derived Cox model: high risk (in blue) or low risk (in red). **C,** Top: Barplot showing the values of the linear predictor estimated from the exome-derived model for each patient: patients with PFS greater than 6 months in blue and lower than 6 months in red. Bottom: Heatmap showing how patients are stratified given the threshold defined in the univariate analysis of each variable selected in the exome-derived model: good prognosis (white) and poor prognosis (black). **D,** Kaplan–Meier estimates for overall survival; patients were stratified according to the value of the linear predictor estimated from the exome-derived Cox model: high risk (in blue) or low risk (in red). **E,** Kaplan–Meier estimates for PFS; patients from the Rizvi and colleagues (2015) cohort were stratified according to the value of the linear predictor estimated from the exome-derived Cox model: high risk (in blue) or low risk (in red). **F** and **G,** Kaplan–Meier estimates for PFS; patients from (**F**) the Hellmann and colleagues (2018) cohort and (**G**) Snyder and colleagues (2017) cohort were stratified according to the value of the linear predictor estimated from the exome-derived Cox model: high risk (in blue) or low risk (in red). All cutoffs were defined with the Cutoff Finder method. *, $P < 0.05$; **, $P < 0.01$; ***, $P < 0.001$; ****, $P < 0.0001$; ns, not significant.

Published OnlineFirst February 1, 2019; DOI: 10.1158/1078-0432.CCR-18-1940

Using Cutoff Finder, a cutoff was chosen on the linear predictor built on all patients with the exome-derived model. This cutoff enables the discrimination of patients with high risk of progression from those with low risk of progression under nivolumab (median PFS: 1.8 vs. NR; log-rank test $P < 0.0001$; $n = 60$; Fig. 4B). Using 6-month PFS as a clinical relevant point, our biomarker classifies 14 of the 15 patients with PFS of more than 6 months as good responders, and only 7 of the 45 patients with PFS less than 6 months are misclassified (leading to a sensitivity of 97% and a positive predictive value of 84%). In the group designated as poor prognosis, we selected one patient with a PFS of more than 6 months and 38 patients with a PFS of less than 6 months (leading to a negative predictive value of 93% and a specificity of 66%; Fig. 4C). By applying the model adjusted on PFS without re-estimation of the coefficients and keeping the same cutoff, we successfully discriminated patients with good and poor OS (median OS: 13.3 vs. NR; log-rank test $P = 0.002$; $n = 60$; Fig. 4D).

Finally, we decided to validate our exome-based model on an external cohort. We used the dataset studied by Rizvi and colleagues (14), which contains 34 patients with lung cancer treated by pembrolizumab. From the 34 patients, 33 were used because the number of neoantigens could not be estimated using pVAC-Seq for one patient. Similarly to the previous cohort, alteration of DNA repair and WNT pathways, the number of infiltrated TCR clones, the number of neoantigens, HLA types, and mutational signatures were determined. On this external cohort treated with another anti-PD-1/PD-L1 interaction inhibitor, we used our nine-variables predictor signature as described above using the same parameters and threshold as for our training cohort. This signature was strongly associated with PFS and could discriminate patients with good and poor PFS (median PFS of 6.3 months vs. NR; log-rank test $P = 0.03$; $n = 33$; Fig. 4E).

To generalize our findings, we finally tested our model on two additional cohorts. We used previously published Hellmann's dataset (25) consisting in 75 patients with NSCLC treated in first-line by nivolumab plus ipilimumab, and the also previously published Snyder's dataset (26), which includes 25 urothelial cancer patients treated with atezolizumab. In both cohorts, a model was adjusted on PFS with the same variables as above. Only the number of TCR clusters was discarded because these data were not available in these cohorts. We showed that our signature model including the same variables had good performances to predict outcome (Supplementary Fig. S4F and S4G), thus generalizing our observations in urothelial cancer and in patients with NSCLC treated in first-line with anti-PD1 plus anti-CTLA4.

Discussion

Immune checkpoint blockade therapies such as anti-PD-1 and anti-PD-L1 mAb have revolutionized the treatment of lung cancer and other cancer types. However, only a fraction of patients benefit from these treatments as monotherapy, and robust predictors of response and understanding of the mechanisms of therapeutic resistance are currently lacking. In this study, we showed that in NSCLCs treated with nivolumab, exome analysis could be used to predict PFS. The information provided by exome analysis allowed a better prediction than clinical data, PD-L1 status, or TMB per Mb information. In addition to an elevated nonsynonymous TMB per Mb and neoantigen rates, which are usually associated with clinical efficacy, some other parameters were studied to better define prognosis. In particular, mutations in DNA repair genetic pathways, TCR clonal restriction, HLA-A*01, the small number of large LOH and deletions, and mutational signatures 1A and 1B were significantly associated with clinical efficacy using univariate Cox models. Using adapted statistical models, we were able to generate a predictive biomarker that includes nine exome-derived variables. Interestingly, when we applied the same pipeline of analysis on another set of patients treated with pembrolizumab and sequenced on another platform using a different technology, we were able to externally validate our biomarker.

Previous studies in this field have analyzed the prognostic role of the most mutated genes to predict response to checkpoint inhibitors (15, 27). Using a similar strategy, we were unable to find any valid predictive biomarkers. Most likely, many mutations in different genes in the same pathway could share similar biological properties; because of the small number of patients in these genetic studies, candidate biomarkers may be selected only by chance. Analyzing mutations at the pathway level may be more relevant and may limit the problem of statistical multitesting.

Rizvi and colleagues also reported that a high fraction of copy number–altered genome is associated with a poor outcome (15). By the same analysis in our series, we also observed that genetic instability and polyclonality were associated with a poor prognosis, but these variables were not selected in the composite variable. Swanton's group reported in patients with lung cancer not treated with immunotherapy that genetic instability and polyclonality are associated with poor prognosis (28), thus suggesting that these genetic variations are more prognostic than they are predictive.

The association of a high nonsynonymous mutation burden per Mb and a high number of neoantigens with prognosis is not surprising and was previously reported by Rizvi and colleagues (14) and Carbone and colleagues (16) in the CheckMate 026 study. The high number of mutations is correlated with the presence of a high number of neoantigens that could be recognized by CD8 T cells and that favor antitumoral immunity. More interestingly, we observed that neoantigens had greater ability to predict PFS than TMB per Mb. Only the number of neoantigens was selected in the composite predictive biomarker; TMB was omitted. In addition, the clinical efficacy of nivolumab correlates with an accumulation of molecular signature 1A and a low accumulation of signature 1B. Both 1A and 1B signatures are characterized by the prominence of C>T substitutions at NpCpG trinucleotides. Because these two signatures are modestly and negatively correlated, it is not surprising that they have opposite clinical outcomes. Signature 4 is frequently observed in lung adenocarcinomas, squamous cell carcinomas, small cell carcinomas, head and neck squamous cell carcinomas, and liver cancers and is considered the smoking signature. Signature 4 is an imprint of the bulky DNA adducts generated by polycyclic hydrocarbons found in tobacco smoke and their removal by transcription-coupled NER (13). This signature 4 is modestly correlated with TMB. However, it is not associated with prognosis in our dataset. In contrast, we observed strong association between signature 4 and PFS in the data of Rizvi and colleagues (not shown). In our data set, 91% of patients were smokers, and thus the smoking signature is overrepresented, which limits the discrimination capacity of this signature.

Interestingly, using the MixCR software we could demonstrate the feasibility of detecting TCR clones in the tumor sample using

Published OnlineFirst February 1, 2019; DOI: 10.1158/1078-0432.CCR-18-1940

exome analysis with a coverage depth of 80× to 100×. Tumeh and colleagues (29) similarly reported in melanoma patients that clonal restriction tested using a dedicated assay (TCR immunoseq) was associated with a better outcome. These data suggest that a preexisting expansion of restricted TCR clones may characterize tumors with antigens recognized by T cells, whereas the presence of multiple clones may characterize tumors with an accumulation of nonspecific T cells with no antitumoral function. We decided to improve the biological classification by including patients with no TCR clones in the tumor with the patients with a high level number of TCR clones using the biological rationale that tumors with poor immunologic responses include tumors with no T-cell infiltration and tumors with polyclonal nonspecific T-cell infiltration. However, this hypothesis is not biologically addressed in the literature at present. The next step will be the characterization, in a tumor sample, of the types of peptides recognized by these clones. This approach could further confirm that these TCR clones recognize shared tumor antigens or neoantigens and confirm the association between TCR clonal restriction and their capacity for tumor antigen detection.

In a more clinically relevant manner, our study is the first to provide a multidimensional prospective analysis of somatic and constitutional exomes of patient treated with anti-PD1 antibody. Our study could generate a composite predictive biomarker of efficacy. This marker could help to identify patients who will have more than 6 month PFS with good sensitivity and specificity. It seemed to be more powerful for detecting patients who will not respond to immunotherapy than TMB or PD-L1 markers that are classically used. This predictive biomarker was also validated in an external cohort previously published by Rizvi and colleagues (14). for patients with lung cancer treated with pembrolizumab. We could also validate our findings in a cohort of NSCLC treated with nivolumab and ipilimumab (25) as well as some urothelial tumors treated with atezolizumab (26). These results suggest that our signature could be generalized to different types of immunotherapy targeting checkpoints, and suggest that it could be tested in other tumor types like urothelial cancer.

However, due to the retrospective design and the low number of patients, this biomarker needs to be validated in further data sets and prospective trials.

Disclosure of Potential Conflicts of Interest

No potential conflicts of interest were disclosed.

Authors' Contributions

Conception and design: C. Truntzer, R. Boidot, F. Ghiringhelli
Development of methodology: C. Richard, C. Truntzer, R. Boidot, F. Ghiringhelli
Acquisition of data (provided animals, acquired and managed patients, provided facilities, etc.): S. Chevrier, A. Lagrange, L. Favier, B. Coudert, L. Arnould, R. Boidot
Analysis and interpretation of data (e.g., statistical analysis, biostatistics, computational analysis): C. Richard, V. Derangère, F. Ledys, C. Truntzer, R. Boidot, F. Ghiringhelli
Writing, review, and/or revision of the manuscript: C. Richard, J.-D. Fumet, L. Arnould, C. Truntzer, R. Boidot, F. Ghiringhelli
Administrative, technical, or material support (i.e., reporting or organizing data, constructing databases): C. Richard, J.-D. Fumet, S. Chevrier, R. Boidot
Study supervision: F. Ghiringhelli, C. Truntzer

Acknowledgments

This work was funded by Georges François Leclerc Cancer Center, INCA (Institut National du Cancer) and Ligue nationale contre le cancer which finance C.R.'s thesis.

The costs of publication of this article were defrayed in part by the payment of page charges. This article must therefore be hereby marked *advertisement* in accordance with 18 U.S.C. Section 1734 solely to indicate this fact.

Received June 18, 2018; revised July 31, 2018; accepted August 22, 2018; published first August 28, 2018.

References

1. Torre LA, Bray F, Siegel RL, Ferlay J, Lortet-Tieulent J, Jemal A. Global cancer statistics, 2012. CA Cancer J Clin 2015;65:87–108.
2. Giroux Leprieur E, Dumenil C, Julie C, Giraud V, Dumoulin J, Labrune S, et al. Immunotherapy revolutionises non-small-cell lung cancer therapy: results, perspectives and new challenges. Eur J Cancer Oxf Engl 1990 2017;78:16–23.
3. Califano R, Kerr K, Morgan RD, Lo Russo G, Garassino M, Morgillo F, et al. Immune checkpoint blockade: a new era for non-small cell lung cancer. Curr Oncol Rep 2016;18:59–63.
4. Borghaei H, Paz-Ares L, Horn L, Spigel DR, Steins M, Ready NE, et al. Nivolumab versus docetaxel in advanced nonsquamous non-small-cell lung cancer. N Engl J Med 2015;373:1627–39.
5. Herbst RS, Baas P, Kim D-W, Felip E, Pérez-Gracia JL, Han J-Y, et al. Pembrolizumab versus docetaxel for previously treated, PD-L1-positive, advanced non-small-cell lung cancer (KEYNOTE-010): a randomised controlled trial. Lancet Lond Engl 2016;387:1540–50.
6. Rittmeyer A, Barlesi F, Waterkamp D, Park K, Ciardiello F, von Pawel J, et al. Atezolizumab versus docetaxel in patients with previously treated non-small-cell lung cancer (OAK): a phase 3, open-label, multicentre randomised controlled trial. Lancet Lond Engl 2017;389:255–65.
7. Lim SH, Sun J-M, Lee S-H, Ahn JS, Park K, Ahn M-J. Pembrolizumab for the treatment of non-small cell lung cancer. Expert Opin Biol Ther 2016;16:397–406.
8. Diggs LP, Hsueh EC. Utility of PD-L1 immunohistochemistry assays for predicting PD-1/PD-L1 inhibitor response. Biomark Res 2017;5:12–20.
9. Grigg C, Rizvi NA. PD-L1 biomarker testing for non-small cell lung cancer: truth or fiction? J Immunother Cancer 2016;4:48–54.
10. Taube JM, Klein A, Brahmer JR, Xu H, Pan X, Kim JH, et al. Association of PD-1, PD-1 ligands, and other features of the tumor immune microenvironment with response to anti-PD-1 therapy. Clin Cancer Res 2014;20:5064–74.
11. Garon EB, Rizvi NA, Hui R, Leighl N, Balmanoukian AS, Eder JP, et al. Pembrolizumab for the treatment of non-small-cell lung cancer. N Engl J Med 2015;372:2018–28.
12. Rizvi NA, Mazières J, Planchard D, Stinchcombe TE, Dy GK, Antonia SJ, et al. Activity and safety of nivolumab, an anti-PD-1 immune checkpoint inhibitor, for patients with advanced, refractory squamous non-small-cell lung cancer (CheckMate 063): a phase 2, single-arm trial. Lancet Oncol 2015;16:257–65.
13. Fehrenbacher L, Spira A, Ballinger M, Kowanetz M, Vansteenkiste J, Mazieres J, et al. Atezolizumab versus docetaxel for patients with previously treated non-small-cell lung cancer (POPLAR): a multicentre, open-label, phase 2 randomised controlled trial. Lancet Lond Engl 2016;387:1837–46.
14. Rizvi NA, Hellmann MD, Snyder A, Kvistborg P, Makarov V, Havel JJ, et al. Cancer immunology. Mutational landscape determines sensitivity to PD-1 blockade in non-small cell lung cancer. Science 2015;348:124–8.
15. Rizvi H, Sanchez-Vega F, La K, Chatila W, Jonsson P, Halpenny D, et al. Molecular determinants of response to anti-programmed cell death (PD)-1 and anti-programmed death-ligand 1 (PD-L1) blockade in patients with non-small-cell lung cancer profiled with targeted next-generation sequencing. J Clin Oncol 2018;36:633–41.

Published OnlineFirst February 1, 2019; DOI: 10.1158/1078-0432.CCR-18-1940

16. Carbone DP, Reck M, Paz-Ares L, Creelan B, Horn L, Steins M, et al. First-line nivolumab in stage IV or recurrent non-small-cell lung cancer. N Engl J Med 2017;376:2415–26.
17. Schwartz LH, Litière S, de Vries E, Ford R, Gwyther S, Mandrekar S, et al. RECIST 1.1-Update and clarification: frrom the RECIST committee. Eur J Cancer Oxf Engl 1990 2016;62:132–7.
18. Budczies J, Klauschen F, Sinn BV, Győrffy B, Schmitt WD, Darb-Esfahani S, et al. Cutoff Finder: a comprehensive and straightforward Web application enabling rapid biomarker cutoff optimization. PloS One 2012;7:e51862.
19. Friedman J, Hastie T, Tibshirani R. Regularization paths for generalized linear models via coordinate descent. J Stat Softw 2010;33:1–22.
20. Kang L, Chen W, Petrick NA, Gallas BD. Comparing two correlated C indices with right-censored survival outcome: a one-shot nonparametric approach. Stat Med 2015;34:685–703.
21. Gyorffy B, Bottai G, Nagy A, Pusztai L, Santarpia L. Immune gene signatures in triple-negative breast cancers characterized by varying levels of chromosomal instability. J Clin Oncol 2017;35:1096–1096.
22. Angelova M, Charoentong P, Hackl H, Fischer ML, Snajder R, Krogsdam AM, et al. Characterization of the immunophenotypes and antigenomes of colorectal cancers reveals distinct tumor escape mechanisms and novel targets for immunotherapy. Genome Biol 2015;16:64–70.
23. Liu C, Peng W, Xu C, Lou Y, Zhang M, Wargo JA, et al. BRAF inhibition increases tumor infiltration by T cells and enhances the antitumor activity of adoptive immunotherapy in mice. Clin Cancer Res 2013;19:393–403.
24. Peng W, Chen JQ, Liu C, Malu S, Creasy C, Tetzlaff MT, et al. Loss of PTEN promotes resistance to T cell-mediated immunotherapy. Cancer Discov 2016;6:202–16.
25. Hellmann MD, Nathanson T, Rizvi H, Creelan BC, Sanchez-Vega F, Ahuja A, et al. Genomic features of response to combination immunotherapy in patients with advanced non-small-cell lung cancer. Cancer Cell 2018;33:843–852.e4.
26. Snyder A, Nathanson T, Funt SA, Ahuja A, Buros Novik J, Hellmann MD, et al. Contribution of systemic and somatic factors to clinical response and resistance to PD-L1 blockade in urothelial cancer: an exploratory multi-omic analysis. PLoS Med 2017;14:e1002309.
27. Miao D, Margolis CA, Gao W, Voss MH, Li W, Martini DJ, et al. Genomic correlates of response to immune checkpoint therapies in clear cell renal cell carcinoma. Science 2018;359:801–6.
28. Jamal-Hanjani M, Wilson GA, McGranahan N, Birkbak NJ, Watkins TBK, Veeriah S, et al. Tracking the evolution of non-small-cell lung cancer. N Engl J Med 2017;376:2109–21.
29. Tumeh PC, Harview CL, Yearley JH, Shintaku IP, Taylor EJM, Robert L, et al. PD-1 blockade induces responses by inhibiting adaptive immune resistance. Nature 2014;515:568–71.

Published OnlineFirst February 1, 2019; DOI: 10.1158/1078-0432.CCR-18-1940

Clinical Cancer Research

Exome Analysis Reveals Genomic Markers Associated with Better Efficacy of Nivolumab in Lung Cancer Patients

Corentin Richard, Jean-David Fumet, Sandy Chevrier, et al.

Clin Cancer Res 2019;25:957-966. Published OnlineFirst February 1, 2019.